Available online at www.sciencedirect.com
ScienceDirect
Journal of Physics and Chemistry of Solids 68 (2007) 716–720
JOURNAL OF PHYSICS AND CHEMISTRY OF SOLIDS
www.elsevier.com/locate/jpcs

Nanostructure materials for destruction of warfare agents and eco-toxins prepared by homogeneous hydrolysis with thioacetamide: Part 1—zinc oxide

Vendula Houšková[a,b,*], Václav Štengl[a], Snejana Bakardjieva[a], Nataliya Murafa[a], Andrea Kalendová[b], František Opluštil[c]

[a]*Institute of Inorganic Chemistry, Academic of Sciences of the Czech Republic, Rez 250 68, Czech Republic*
[b]*Faculty of Chemical Technology, Institute of Polymeric Materials, University of Pardubice, nám.Cs.Legií 562, Pardubice 532 10, Czech Republic*
[c]*Military Technical Institute of Protection, Veslarska 230, Brno 628 00, Czech Republic*

Abstract

Zinc sulphide (ZnS) nanoparticles were prepared by homogeneous hydrolysis of zinc sulphate and thioacetamide (TAA) at 80 °C. After annealing at temperature above 400 °C in oxygen atmosphere, zinc oxide (ZnO) nanoparticles were obtained. The ZnS and ZnO nanoparticles were characterized by X-ray diffraction (XRD), scanning electron microscopy (SEM), high resolution transmission microscopy (HRTEM), selected area electron diffraction (SAED), by BET and BJH methods used for surface area and porosity determination. The photocatalytic activity of the as-prepared ZnO samples was determined by the decomposition of Orange II in the aqueous solution under UV irradiation of 365 nm of wavelength.

Keywords: C. X-ray diffraction

1. Introduction

Homogeneous hydrolysis with urea as a precipitate agent can be used for preparation of oxo-compounds, such as metal oxides and hydroxides, or precursor on base mixed oxo-hydroxides. The urea method is based on thermal decomposition of urea at a temperature higher than 60 °C [1,2]:

$$(NH_2)_2CO + H_2O \rightarrow CO_2\uparrow + 2NH_4OH \quad (1)$$

$$NH_4OH + H_2O \rightarrow NH_4^+ + 2OH^- \quad (2)$$

$$Me^{2+} + OH^- \rightarrow Me(OH)_2 \quad (3)$$

On heating aqueous solution of urea, the stoichiometry of urea hydrolysis can be described by Eq. (4):

$$OC(NH_2)_2 + H^+ + 2H_2O \rightarrow HCO_3^- + 2NH_4^+ \quad (4)$$

According to Soler-Illia [3], the hydrolysis of urea takes place in two steps:

$$OC(NH_2)_2 \rightarrow OCN^- + NH_4^+ \quad (5)$$

$$OCN^- + H^+ + 2H_2O \rightarrow HCO_3^- + 2NH_4^+ \quad (6)$$

The first step, the reversible formation of ammonium cyanate is followed by the irreversible hydrolysis of cyanate ions. During the decomposition of urea, the NH_4^+ ions are formed and the consumption of H^+ results in increase of pH in the solution. After reaching the pH value necessary for precipitation of the hydroxides, precipitates of insoluble material start to form [3]. Contrary to the heterogeneous precipitation method, when acidic metal salt solution is mixed with the basic neutralizing agent, much milder concentration gradients occur during the homogeneous

*Corresponding author. Faculty of Chemical Technology, Institute of Polymeric Materials, University of Pardubice, nám.Cs.Legií 562, Pardubice 532 10, Czech Republic. Tel.: 420 2 6617 3534; fax: 420 2 2094 0257.
E-mail address: houskova@iic.cas.cz (V. Houšková).

0022-3697/$ - see front matter © 2007 Elsevier Ltd. All rights reserved.
doi:10.1016/j.jpcs.2006.12.012

precipitation, resulting in significantly different properties of the precipitation product.

In the same way as urea method, homogeneous precipitation of metal sulphides by thermal decomposition of thioacedamide (TAA) can be used [4]. Thioacetamide at a temperature higher than 60 °C in acidic solution released hydrogen sulphide:

$$CH_3CSNH_2 + H_2O \rightarrow CH_3CONH_2 + H_2S \quad (7)$$

$$H_2S + H_2O \rightarrow HS^- + H_3O^+ \quad (8)$$

$$Me^{2+} + HS^- \rightarrow MeS + H^+. \quad (9)$$

The reaction products are nanosized spherical particles with a well-developed microstructure, but different from homogeneous precipitation with urea. These products with high specific surface area are very well washed and filtered.

2. Experimental

2.1. Synthesis of samples

All used chemicals, zinc sulphate and TAA, were of analytical grade and were supplied by Fluka. 1 M of $ZnSO_4 \cdot 7H_2O$ was dissolved in 4 L of distilled water and was added 1 M of thioacetamide. The reaction mixture was adjusted to the pH = 2 with sulphuric acid. The reaction mixture was heated at temperature 80 °C under stirring for 4 h. Thus, synthesized zinc sulphide has been washed by distilled water with decantation, filtered off and dried at 105 °C in furnace. After atmosphere annealing in temperature range 400–800 °C in oxygen atmosphere for 1 h, six fine ZnO/ZnS powders denoted as SIS 7_200, SIS 7_400, SIS 7_500, SIS 7_600, SIS 7_700, SIS 7_800 was synthesized.

2.2. Characterization methods

The surface area of the samples was determined from nitrogen adsorption–desorption isotherms at liquid nitrogen temperature using a Coulter SA3100 instrument with outgas 15 min at 120 °C. The BET method was used for surface area calculation [5], and the pore size distribution (pore diameter and pore volume of the samples) was determined by the BJH method [6].

Transmission electron micrographs (TEM and HRTEM) were obtained by using two instruments, namely Philips EM 201 at 80 kV and JEOL JEM 3010 at 300 kV (LaB_6 cathode). A copper grid coated with a holey carbon support film was used to prepare samples for the TEM observation. A powdered sample was dispersed in ethanol and the suspension was treated in ultrasonic bath for 10 min.

Scanning electron microscopy (SEM) studies were performed using a Philips XL30 CP microscope equipped with EDX, Robinson, SE and BSE detectors. The sample was placed on an adhesive C slice and coated with Au–Pd alloy 10 nm thick layer.

X-ray powder diffraction patterns were obtained on a Siemens D5005 instrument using CuKα radiation (40 kV, 30 mA) and diffracted beam monochromator. Qualitative analysis was performed with the Eva Application and the Xpert HighScore using the JCPDS PDF-2 database.

Kinetics of the photocatalytic degradation, as well as mineralization of 25 ml 0.25 mM Orange II [7] and 200 mL solutions with particles of zinc oxide (200 mg/L), were measured. Quartz water-jacketed laboratory photoreactor, magnetically stirred and continuously irradiated with one "black light" lamp ($\lambda = 365$ nm, $I_0 = 5{,}3 \times 10^{-5}$ einstein/dm^3s), was used. The laboratory irradiation experiments were performed in a self-constructed photoreactor. It consists of two coaxial quartz tubes placed in the middle of a steel cylinder with an aluminium foil covering its inner wall. The inner quartz tube (diameter 24 mm, length 300 mm) was filled with the investigated suspension (70 mL) and magnetically stirred. Cooling water was circulating between the inner and the outer quartz tubes to maintain a constant temperature of 20 °C. The used source of UV irradiation was a high-pressure mercury lamp enclosed in a glass filter bulb whose emission consists of 93% of 365 nm radiation. It was placed close to the quartz tubes. By the means of the ferrioxalate actinometry, an average light intensity entering the volume of 50–70 mL of the irradiated solution was determined as $I_0 = 5.3 \times 10^{-5}$ einstein/dm^3s. The irradiated solution was sucked from the reactor with a peristaltic pump through a flow cuvette back to the reactor. The concentration of Orange II was determined by measuring absorbance at 480 nm with VIS spectrophotometer ColorQuestXE.

3. Results and discussion

3.1. X-ray diffraction (XRD)

The pattern of XRD for sample SIS7 prepared by homogeneous hydrolysis of zinc (II) sulphate with TAA is shown in Fig. 1a. It shows that the nano-crystals exhibit a zinc blende crystal structure (ZnS, PDF 05-0566).

It is known that decrease in particle size results in a broadening of the diffraction peaks. From full-width at half-maximum (FWHM) of the strongest diffraction peak in plane (1 1 1), the mean particle's size t in diameter was determined from the peak half-width B by Scherrer formula [8]

$$t = \frac{k\lambda}{B \cos \Theta} \quad (10)$$

where k is a shape factor of the particle ($k = 1$ if the spherical shape is assumed), λ and Θ are the wavelength and the incident angle of the X-rays, respectively. The peak width was measured at half of the maximum intensity. Fig. 1b–d shows the XRD patterns of sample SIS7 annealed in the temperature interval 200–500 °C in oxygen atmosphere.

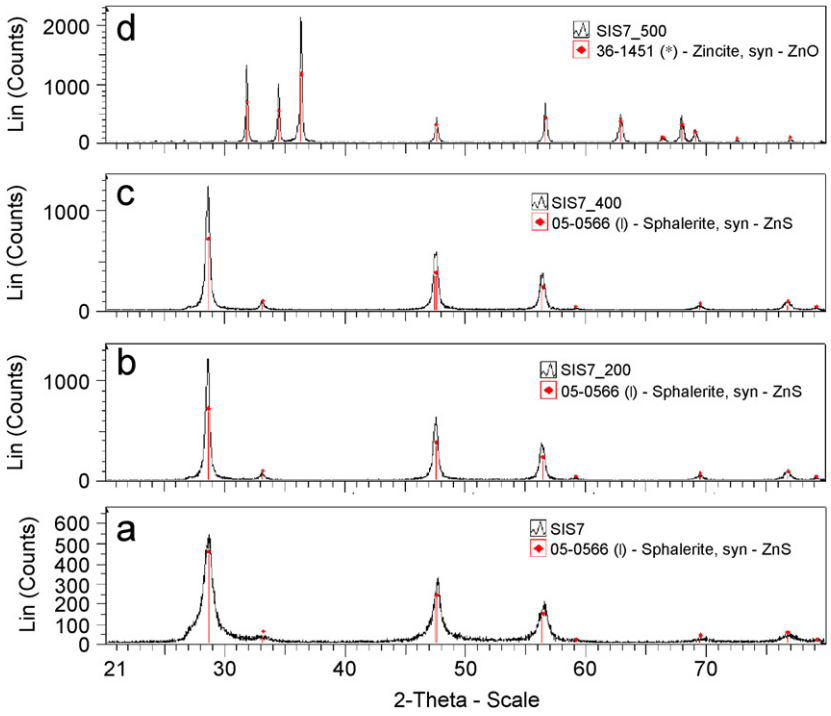

Fig. 1. XRD patterns of the ZnS (a) and ZnS samples annealed at 200 °C (b), 400 °C (c), 500 °C (d).

Table 1
Characteristics of prepared samples

Sample	Heat. temp. (°C)	RTG	t (nm)	BET ($m^2 g^{-1}$)	Total pore area (nm)	Total pore volume (cm^3/g)	K (min^{-1})
SIS7	0	ZnS	6.2	76.8	1.718	0.02	—
SIS7_200	200	ZnS	18.0	153.5	1.536	0.06	—
SIS7_400	400	ZnS	19.9	101.9	1.527	0.01	0.0005
SIS7_500	500	ZnO	41.8	50.54	1.530	0.02	0.0043
SIS7_600	600	ZnO	48.7	35.9	1.527	0.01	0.0079
SIS7_700	700	ZnO	74.2	31.3	1.527	0.01	0.0379
SIS7_800	800	ZnO	75.9	13.4	1.527	0.01	0.0196
Deggusa P25	—	TiO_2	—	50	—	—	0.0222

As shown in XRD patterns, zinc blende structure was transformed into zincite (ZnO, PDF 36-1451) at a temperature higher than 400 °C. It suggested that the zinc sulphide nanoparticles were oxidized into ZnO nanoparticles.

Refering to Fig. 1, the strongest diffraction peak in plane (1 0 1) consists of the standard zinc oxide powder diffraction file. From FWHM values of zinc oxide (1 0 1) plane diffraction peak, the particle diameters were obtained. Table 1 shows the result calculated from Debeye–Scherrer formula. In Table 1, we find that the particle size (t) increases with the increasing annealing temperature.

3.2. Surface area and porosity

In Table 1 is shown the surface area (BET), the pore distribution and total volume of pores related to mass (porosity) of samples obtained at various heating temperatures. These show that the specific surface of zinc sulphide (samples SIS7, SIS7_200) grows with increase in temperature. At temperature of 400 °C (sample SIS7_400), recrystallization process takes place and the specific surface area is decreased. With increasing temperature above 400 °C (samples SIS7_500—SIS7_800), the specific surface area goes on to decreasing.

The pore distribution calculated by BJH method confirms that the samples of zinc sulphite and zinc oxide are microporous with pore sizes in range 2–6 nm. Variable annealing temperature did not change the total pore area and the total pore volume (Table 1).

3.3. High resolution transmission electron microscopy (HRTEM) and ED

Image processing analysis of HRTEM micrograph is a useful method in refinement of microstructure in the sense

that we can more accurately analyse the grain's size and grain's boundaries. Furthermore, from Fourier transform (FFT), it is possible to determine and to index crystallographic planes and find orientations of nanoparticles. HRTEM micrograph (Fig. 2) shows that the lattice spacing of approximately 0.347 nm between adjacent lattice planes corresponds to the distance between [2 0 0] crystal planes. From the database (PDF 05-0566, JCPDS PDF2, 2001), it follows that the lattice spacing $d = 0.347$ corresponds to the [2 0 0] diffraction line of sphalerite.

The HRTEM image of ZnO crystallites (see Fig. 3) obtained at annealing sample SIS 7 at temperature 700 °C in oxygen atmosphere (sample SIS7_700) shows two types of domains corresponding to ZnO space-group Fm-3m. The face-centred cubic unit cell has been used to index the ED pattern (calculated by FFT) inserted in Fig. 3. The motive in Fig. 3c corresponding to plane [0 0 1] and motive in Fig. 3d correspond to plane [1 1 1]. The particle size calculated from HRTEM is similar to that obtained by the X-ray powder diffraction method.

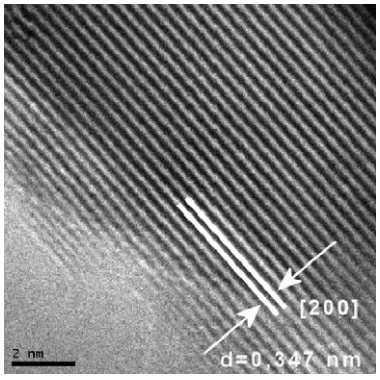

Fig. 2. HRTEM micrographs of sphalerite prepared by homogeneous precipitation with TAA denoted as SIS7, magnification 25,000.

3.4. Scanning electron microscopy

It is apparent that the product of homogeneous precipitation of thioacetamide and zinc sulphate consists of approximately by spherical round particle agglomerates of diameter about 1 μm (Fig. 4), which are formed from spherical particles of 6 nm joined to the chains, after oxidation agglomerates and chains of particles have disintegrated and particle cluster of approximately size 10 nm has been formed. With increasing annealing temperature, the agglomerate size decreases.

3.5. Photocatalytic activity

It follows from Fig. 5 that the zincite particles show good photocatalytic properties for the decomposition of Orange II in an aqueous solution under UV radiation. The time dependences of Orange II decomposition were fitted by

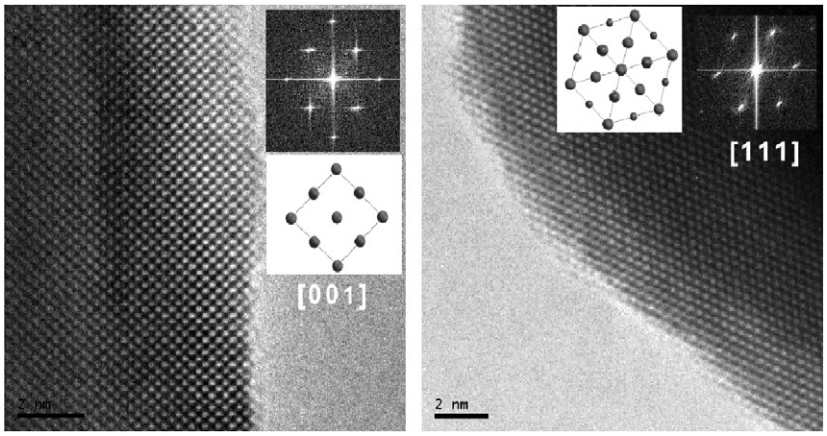

Fig. 3. HRTEM micrographs of zincite prepared by annealing of the sample denoted as SIS7 at temperature of 600 °C for 2 h in oxygen atmosphere, magnification 100,000.

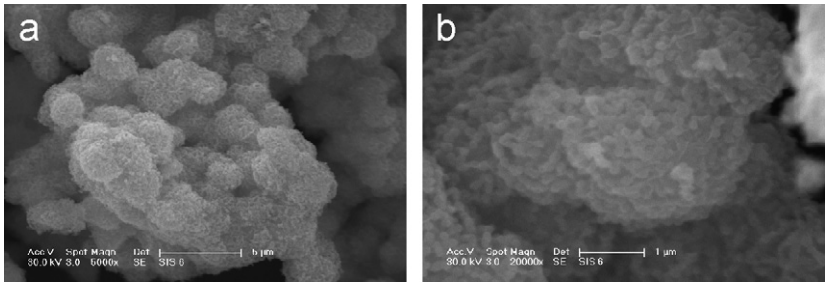

Fig. 4. SEM micrographs of particles prepared by homogeneous hydrolysis of zinc sulphate and thioacetamide (TAA) at temperature of 80 °C (a, b).

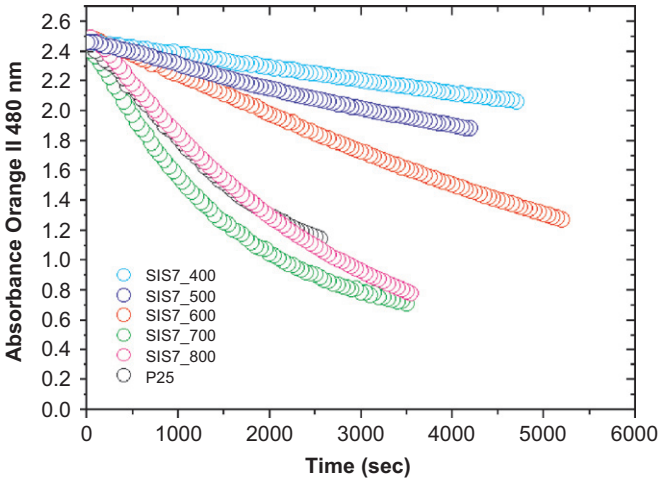

Fig. 5. Photocatalytic decomposition of Orange II on zinc sulphite (ZnS) samples annealed at temperature upper 400 °C (SIS7_400-800) and on the standard photocatalyst Degussa (P25).

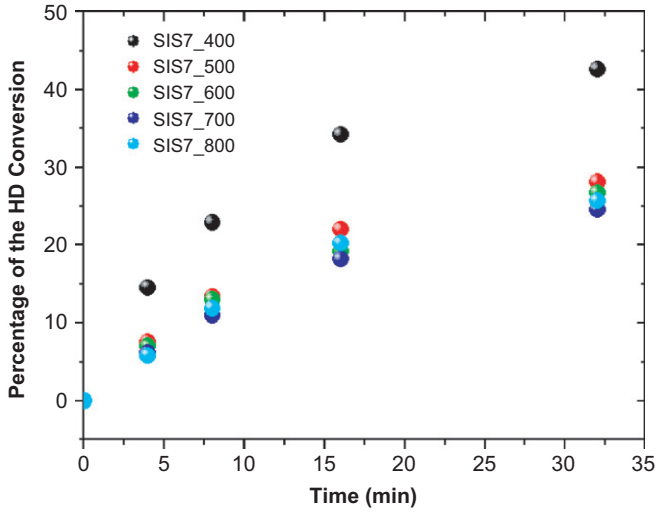

Fig. 6. Decomposition of sulphur mustard on prepared samples with time.

using Eq. (11) for the first-order kinetics reaction [9]:

$$\frac{d[O_2]}{dt} = k(a_0 - [O_2]) \quad (11)$$

where $[O_2]$ is concentration of Orange II, a_0 is initial concentration of Orange II and k is rate constant.

On the basis of the results in Table 1, we found that the rate constant k of the mineralization of Orange II increases with annealing temperature. Probably, well crystallized nanoparticles, with average size 40–75 nm and with perfect crystal structure, improve the photocatalytic activity of ZnO particles. The corresponding kinetic curve of the standard photocatalyst P25 (Degussa) is included.

3.6. Method of disintegration of warfare agents

The samples of zinc oxide were evaluated for their ability to degrade chemical warfare agents (sulphur mustard gas) to nontoxic products. The respective detoxification capabilities of evaluated samples were expressed as percentages of the sulphur mustard (HD) conversion (see Fig. 6). Good results were obtained by the decomposition on zinc oxide annealed at temperature 400 °C (sample SIS7_400), where conversion comes to 42%. With increasing annealing temperature, the decomposition of warfare agents decreases because of the lower specific surface area of samples.

4. Conclusion

The spherical particles of zinc sulphide was prepared by homogeneous hydrolysis of zinc(II) sulphate in aqueous solution at temperature of 80 °C with thioacetamide. The ZnS was annealed in oxygen atmosphere in temperature range 200–800 °C and converted to ZnO. The sample heated at temperature 700 °C exhibited a good photocatalytic activity, $k = 0.0379\,min^{-1}$ (k for P25 Degussa is $0.0222\,min^{-1}$). The sample heated at temperature of 400 °C in oxygen atmosphere efficiently decomposes chemical warfare agent such as mustard gas.

Acknowledgements

The work was supported by the Academy of Sciences of the Czech Republic (Project No. AV0Z40320502).

References

[1] M. Ocana, M.P. Morales, C.J. Serna, Homogeneous precipitation of uniform α-Fe_2O_3particles from iron salts solutions in the presence of urea, J. Colloid Interface Sci. 212 (1998) 317–323.
[2] K. Ch. Song, Y. Kang, Preparation of high surface area tin oxide powders by a homogeneous precipitation method, Mater. Lett. 42 (2000) 283–289.
[3] G. Soler-Illia, M. Jobbagy, R.J. Candal, A.E. Regazzoni, M.A. Blesa, The sythesis of metal oxide particles from aqueous media: the controlled hydrolysis method, J. Dispersion Sci. Technol. 19 (1998) 207–229.
[4] T. Nomura, Y. Kousaka, M. Alonso, M. Fukunaga, Precipitation of zinc sulfide particles from homogeneous solutions, J. Colloid Interface Sci. 223 (2000) 179–184.
[5] S. Brunauer, P.H. Emmett, E. Teller, Adsorption of gases in multimolecular layers, J. Am. Chem. Soc. 60 (1938) 309.
[6] E.P. Barret, L.G. Joyner, P.P. Halenda, The determination of pore volume and area distributions in porous substances, J. Am. Chem. Soc. 73 (1951) 373.
[7] M. Stylidi, D.I. Kondarides, X.E. Verykios, Visible light-induced photocatalytic degradation of acid Orange 7 in aqueous TiO_2 suspensions, Appl. Catal B: Environ. 47 (2004) 189–201.
[8] A.L. Patterson, The Scherrer formula for X-ray particle size determination, Phys. Rev. 56 (1939) 978–982.
[9] K. Macounová, H. Krýsová, J. Ludvík, J. Jirkovský, Kinetics of photocatalytic degradation of diuron in aqueous colloidal solution of Q-TiO_2 particles, J. Photochem. Photobiol. A: Chem. 156 (2003) 273–282.